COMBINED TREE SEGMENTATION AND STEM DETECTION USING FULL WAVEFORM LIDAR DATA

J. Reitberger [a, *], P. Krzystek [a], U. Stilla [b]

[a] Dept. of Geoinformatics, Munich University of Applied Sciences, 80333 Munich, Germany
(reitberger, krzystek)@fhm.edu
[b] Photogrammetry and Remote Sensing, Technische Universitaet Muenchen, 80290 Munich, Germany
stilla@tum.de

Commission III, WG III /3

KEY WORDS: LIDAR, Analysis, Segmentation, Forestry, Vegetation

ABSTRACT:

The study highlights a new method for the delineation of tree crowns and the detection of stem positions of single trees from dense airborne LIDAR data. At first, we combine a method for surface reconstruction, which robustly interpolates the canopy height model (CHM) from the LIDAR data, with a watershed algorithm. Stem positions of the tallest trees in the tree segments are subsequently derived from the local maxima of the CHM. Additional stem positions in the segments are detected in a 3-step algorithm. First, all the points between the ground and the crown base height are separated. Second, possible stem points are found by hierarchically clustering these points. Third, the stem is reconstructed with a robust RANSAC-based adjustment of the stem points. The method was applied to small-footprint full waveform data, which have a point density of 25 points per m^2. The detection rate for coniferous trees is 61 % and for deciduous trees 44 %, respectively. 7 % of the detected trees are false positives. The mean positioning error is 0.92 cm, whereas the additional stem detection improves the tree position on average by 22 cm. The analysis of waveform data in the tree structure shows that the intensity and pulse width discriminate stem points, crown points and ground points significantly. Moreover, the mean intensity of stem points turned out to be the most salient feature for the discrimination of coniferous and deciduous trees.

1. INTRODUCTION

Laser scanning has been widely used in mapping the Earth's surface and especially in forest application. Conventional LIDAR, which records the first and last pulse, was successfully applied to retrieve forest parameters like tree height, crown diameter, number of stems, stem diameter and basal area on the tree level (Hyyppä et al., 2004). Also, tree species classification became feasible with first/last pulse scanning systems providing high point density (Holmgren et al., 2004; Heurich, 2006; Brandtberg, 2007). Recently, studies reported about the successful application of novel small footprint full waveform systems to DTM generation (Doneus et al., 2006) or to tree species classification (Reitberger et al., 2006) using advantageously the intensity and the pulse width.

Approaches to tree species classification are usually based on a single tree segmentation that delineates the tree crown from the outer geometry of the forest surface. The methods have in common to reconstruct – at least locally – the CHM to find the local maximum as the best guess for the stem position and to delineate a segment polygon as the tree crown. For example, the CHM is locally interpolated from the highest laser reflections (Hyyppä et al., 2001), derived with the active contour algorithm (Persson et al., 2002), or is interpolated with special gridding methods (Solberg et al., 2006). Stem positions are determined from the interpolated CHM at the highest positions (Solberg et al., 2006) or from a special local tree shape reconstruction (Brandtberg, 2007). Tree crowns are typically derived with the watershed algorithm (Pyysalo et al., 2002), by a slope-based segmentation (Persson et al., 2002; Hyyppä et al., 2001) or by a region growing method that starts from local surface maximums and finds crown polygons optimised in shape (Solberg et al., 2006).

The drawback of the segmentation methods is that they solely base on the CHM, which is reconstructed from the raw data in an interpolation process that smoothes the data to some extent. The degree of smoothing directly affects the success rate in terms of false positives and negatives. Moreover, in some cases neighbouring trees do not appear as two clear local maximums. Thus, approaches that solely use the CHM will be restricted in the success rate anyway, especially in heterogeneous forest types where groups of trees grow close together. So far, little focus has been given to reconstruct trees using information like laser hits on the stems or the reflectance, mainly because of the low spatial point density and the lack of information about the reflecting characteristics of the tree structure. Detected tree stems could be used to improve the CHM-based segmentation in terms of the detection rate and the position of the trees. Moreover, the analysis of the internal tree reflecting characteristics will gain more insight about salient tree features which are significant for instance for tree species classification or DTM generation. New full waveform systems have the potential to overcome these drawbacks since they detect significantly more reflections in the tree crown and provide the intensity and the pulse width as reflecting parameters.

The objective of this paper is (i) to present a method that segments single trees with a robust surface reconstruction method in combination with the watershed algorithm, (ii) to introduce a novel approach to stem detection that clusters hierarchically potential stem reflections and reconstructs the stem with a RANSAC-based adjustment, (iii) to show how the detection rate and position of single trees is improved, and (iv) to analyse the distribution of the parameters intensity and pulse width of the reflections in the tree structure.

* Corresponding author.

The paper is divided into five sections. Section 2 focuses on the segmentation of the single trees and the reconstruction of the tree stems. Section 3 shows the results which have been obtained from full waveform data acquired in May 2006 by the Riegl LMS-Q560 scanner in the Bavarian Forest National Park. Finally, the results are discussed with conclusions in sections 4 and 5.

2. METHODOLOGY

2.1 Decomposition of full waveform data

Let us assume that full waveform LIDAR data have been captured in a region of interest (ROI). A single waveform is decomposed by fitting a series of Gaussian pulses to the waveform which contains N_R reflections (Figure 1).

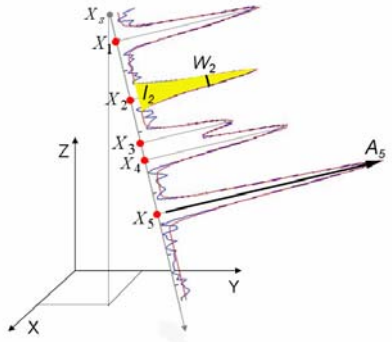

Figure 1. 3D points and attributes derived from a waveform

The vector $\boldsymbol{X}_i^T = (x_i, y_i, z_i, W_i, I_i)(i = 1,..., N_R)$ is provided for each reflection i with (x_i, y_i, z_i) as the 3D coordinates of the reflection. Additionally, the points $\boldsymbol{X}_i$ are given the width $W_i = 2 \cdot \sigma_i$ and the intensity $I_i = \sqrt{2 \cdot \pi} \cdot \sigma_i \cdot A_i$ of the return pulse with σ_i as the standard deviation (= half pulse width at $A_i / \sqrt{e}$) and A_i as the amplitude of the reflection i (Reitberger et al., 2006; Jutzi and Stilla, 2005). Note that basically each reflection can be detected by the waveform decomposition. This is remarkable since conventional LIDAR systems – recording at most five reflections – have a dead zone of about 3 m which makes these systems effectively blind after a reflection.

Class	Single	First	Middle	Last
Definition	N_R=1 i=1	$N_R \geq 2$ i=1	$N_R \geq 3$ i=2,…, N_R-1	$N_R \geq 2$ i=N_R

Table 1. Subdivision of points into classes in dependence on the number of reflections N_R and the position i of the reflection in the waveform

The sensor data are calibrated by referencing W_i and I_i to the pulse width W^e and the intensity I^e of the emitted Gaussian pulse and correcting the intensity with respect to the run length s_i of the laser beam and a nominal distance s_0.

$$W_i^c = W_i / W^e \quad (1)$$

$$I_i^c = (I_i \cdot s_i^2) / (I^e \cdot s_0^2) \quad (2)$$

Note that the correction assumes a target size larger or equal to the footprint (Wagner et al., 2006). The points from a waveform are subdivided into 4 point classes depending on the number of reflections within a waveform (Table 1).

2.2 Segmentation

The segmentation of the tree crowns is achieved by deriving the CHM from 3D points which are best representing the outer tree crown geometry. The ROI is subdivided into a grid having a cell spacing of cp and N_C cells. Within each cell of size cp^2, the highest 3D point is extracted and corrected with respect to the ground level z_j^{ground}, i.e. $z_j^{CHM} = z_j - z_j^{ground} (j = 1,..., N_C)$. The ground level z_j^{ground} is estimated from a given DTM by bilinear interpolation. In the next step, all the highest 3D points $\boldsymbol{X}_j^T = (x_j, y_j, z_j^{CHM})(j = 1,..., N_C)$ of all N_C cells are robustly interpolated in a grid that has N_X and N_Y grid lines and a grid width gw. The special adjustment approach (Krzystek et al., 1992) interpolates the $N_{CHM} = N_X * N_Y$ grid points $\boldsymbol{X}_{Int\ j}^{CHM\ T} = (x_{Int\ j}^{CHM}, y_{Int\ j}^{CHM}, z_{Int\ j}^{CHM})(j = 1,..., N_{CHM})$ and filters the 3D points $\boldsymbol{X}_j$ in a 2-phase iterative Gauß-Markoff process. Thanks to constraints on the curvature and torsion of the surface, the interpolation smoothes and regularises the surface in case of an ill-posed local situation. The iterative adjustment scheme is similar to an edge preserving filter that discards outliers, closes gaps in the surface if no 3D points could be found in the cells, and preserves surface discontinuities. The result is a smoothed CHM having N_{CHM} equally spaced posts. Finally, the tree segments are found by applying the watershed algorithm (Vincent and Soille, 1991) to the CHM. The local maximums of the segments define the N_{seg} tree positions $(X_{stem\ i}^{CHM}, Y_{stem\ i}^{CHM})(i = 1,..., N_{seg})$.

2.3 Stem detection

Tree stems in the individual tree segments are detected in a 3-step procedure:

Step 1: The N_S points $X_j^{Seg} (j = 1,..., N_S)$ within a tree segment are cleared from ground points by discarding all points within a given height bound $Z_{threshold}$ = 1 m to the DTM.

Step 2: The goal of the second step is to derive the crown base height h_{base} of the tree in order to subdivide the tree into the stem area and the remaining crown area. This coarse tree subdivision is achieved by (i) splitting the tree into l layers with height of 0.5 m, (ii) calculating the number of points n_i per layer, (iii) forming the vector $\boldsymbol{N_P} = \{n_i / N_S\}(i = 1,..., l)$, (iv) smoothing $\boldsymbol{N_P}$ with a 3x1 Gaussian filter and, finally, (v) defining h_{base} as the height that corresponds to 0.15 % of the total number of points per segment. All the N_{stem} points below h_{base} are potential stem points. Note that the remaining points can result from one or even several stems or from the understorey. The following hierarchical clustering scheme is applied to these points after calculating the Euclidian distance matrix $D_{stem} = \{ d_{ij} = \sqrt{(x_i - x_j)^2 + (y_i - y_j)^2}$; $i=1,...,N_{stem}$; $j=1,...,N_{stem}$; $i \# j\}$ (Heijden et al., 2004).

1. Assign each point to its own cluster, resulting in N_{stem} clusters.
2. Find the closest pair of clusters and merge them into one cluster. The number of clusters reduces by one.

3. Compute the distance d between the new clusters and each of the old clusters.
4. Repeat steps 2 and 3 until all items are clustered into a single cluster of size N_{stem} or a predefined number of clusters is reached.

In this clustering process the distance between two clusters C_i and C_j is defined as the shortest distance from any point in one cluster to any point in the other cluster. The clustering yields a dendrogram which shows at which distance the clusters are grouped together. By defining a minimum distance d_{min} between the cluster centres the number of clusters $N_{cluster}$ is selected. The value of d_{min} must be larger than the maximum distance of stem points and smaller than the distance of points belonging to different stems. A value of 1.2 m was found to be most useful.

Step 3: The final finding of the stems is achieved by applying a RANSAC-based 3D line adjustment to all the $N_{cluster}$ clusters and labelling all 3D lines with an incident angle smaller than $\alpha = 7^0$ and a minimum number of 3 points as stems g_{stem}. This robust procedure eliminates clusters that result from the understorey and do not show a vertical main direction. Also, it cleans the cluster points from non-stem points. The detected stem positions $(x_{stem}^{det}, y_{stem}^{det}) = \{DTM \cap g_{stem}\}$ are calculated as the intersection of the stem g_{stem} with the DTM. Note that several stems can be found within a tree segment.

3. EXPERIMENTS

3.1 Material

Experiments were conducted in the Bavarian Forest National Park which is located in south-eastern Germany along the border to the Czech Republic (49° 3' 19" N, 13° 12' 9" E). 11 sample plots with an area size between 1000 m^2 and 3600 m^2 and a mean tree density of 390 trees per ha were selected in the mixed mountain forests. The plots comprise forest in the regeneration phase, the late pole phase and the optimal phase. Reference data for all trees with diameter at breast height (DBH) larger than 10 cm have been collected in May 2006 for 438 Norway spruces (*Picea abies*), 477 European beeches (*Fagus sylvatica*), 74 fir trees (*Abies alba*), 20 Sycamore maples (*Acer pseudoplatanus*) and 3 Norway maples (*Acer platanoides*). Several tree parameters like the DBH, total tree height, stem position and tree species were measured and determined with the help of GPS, tacheometry and the 'Vertex' III system. A DTM with a grid size of 1 m and an absolute accuracy of 25 cm was available (Heurich, 2006). Full waveform data have been collected by Milan Flug GmbH with the Riegl LMS-Q560 scanner in May 2006 after snowmelt but prior to foliation with an average point density of 25 points/m^2. The vertical sampling distance was 15 cm, the pulse width at half maximum reached 4 ns and the laser wavelength was 1550 nm. The flying altitude of 400 m resulted in a footprint size of 20 cm.

3.2 Single tree detection

The procedures for segmentation and subsequent stem detection were applied to all the plots in a batch procedure without any manual interaction. Figure 2 shows a typical sample area containing several coniferous trees. The tree tops derived from the local maximums of the CHM correspond in some cases with the reference trees reasonably. However, some tree tops are deviating considerably from the true position. Moreover, some segments contain more than one reference tree. The main reasons are that (i) a group of trees form locally a well-defined maximum and (ii) the surface reconstruction smoothes too much so that neighbouring trees cannot be isolated. In both cases the single trees are not detected and hence the segment represents a group of trees rather than a single tree.

The stem detection takes advantage of additional high-density point information the waveform decomposition provides underneath the CHM. In case that only sparse understorey is below the base height stem points are successfully detected by the hierarchical clustering and the RANSAC-based stem reconstruction. Figures 3a and 3b show the stem points for the segment in the centre of Figure 2 found by the clustering scheme given in section 2.3. The two stems are clearly isolated by applying the angle constraint of 7^0 to the stems approximated with RANSAC. Moreover, the single stem position derived from the CHM maximum is significantly improved by the new stem position. Thus, the stem detection provides additional single trees that constitute no local maximum in the CHM and improves the position of trees derived from the CHM maximum in the majority of cases.

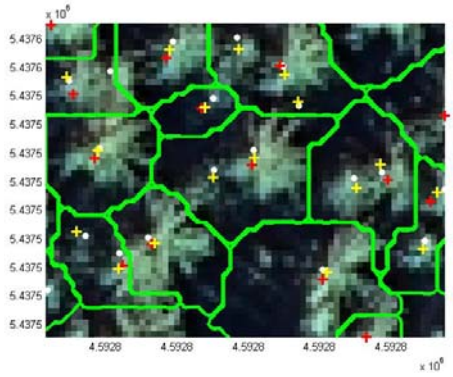

Figure 2. Orthophoto of sample area with segments (green lines), reference coniferous trees (white dots), detected stems (yellow crosses) and the local CHM maximums (red crosses)

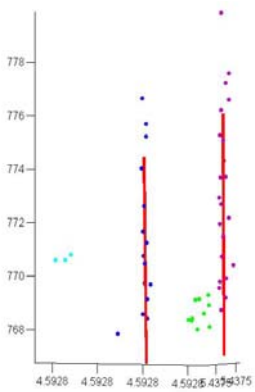

Figure 3a. Stem point clusters and stems reconstructed with RANSAC

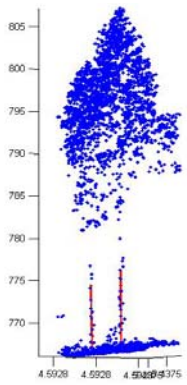

Figure 3b. The neighbouring trees and the reconstructed stems

Let us now evaluate the accuracy and reliability of the presented method. Table 2 contains the percentage of detected trees for all the plots. The trees are subdivided into 3 layers with respect to the mean height h_{top} of the 100 highest trees per ha. The lower layer contains all trees below 50 % of h_{top}, the intermediate layer refers to all trees between 50 % and 80 % of h_{top}, and, finally, the upper layer contains the rest of the trees.

Number of reference trees in lower layer		229
Number of reference trees in intermediate layer		161
Number of reference trees in upper layer		622
Percentage of deciduous [%]		49
Without "stem detection"	Detected trees lower layer [%]	3
	Detected trees intermediate layer [%]	13
	Detected trees upper layer [%]	74
	Total number of detected trees [%]	49
	False detected trees [%]	5
With "stem detection"	Detected trees lower layer [%]	3
	Detected trees intermediate layer [%]	21
	Detected trees upper layer [%]	78
	Total number of detected trees [%]	53
	False detected trees [%]	7

Table 2. Detection of trees in the reference plots

Mean positioning error	Without "stem detection"	With "stem detection"
Coniferous	0.80 m	0.70 m
Deciduous	1.65 m	1.22 m
Total	1.16 m	0.92 m

Table 3. Accuracy of the tree position

At first, we focus on the detection rate of trees that are derived from the CHM without stem detection and hence refer to a local maximum in the CHM. The overall detection rate of 74 % evidences that most of the trees are detected in the upper layer. In comparison, in the intermediate and lower layer the detection rate is considerably smaller. Especially, in the lower layer only a few trees can be found since most of these trees are covered by taller trees. The mean number of false detected trees amounts to 5 % and indicates a remarkable reliability. When applying the stem detection we get an overall improvement of the detection rate in the intermediate layer of 8 % and in the upper layer of 4 %. However, no improvement is achieved in the lower layer since (i) laser hits at the stem of small trees happen rarely, (ii) the base height h_{base} is inaccurate for trees beneath taller trees, and (iii) some trees have no clear h_{base} since their green branches start close to the ground. Additionally, we found that the detection rate is on average for coniferous trees 61 % and for deciduous trees 44 %, respectively. Finally, Table 3 shows the absolute positional improvement of the trees derived from the stem positions $(x_{stem}^{det}, y_{stem}^{det})$ and the position of the reference trees. As expected, the mean positioning error of deciduous trees gets better by 26 %, which corresponds to 43 cm. The overall improvement of the tree position amounts to 24 cm, which is equivalent to 21%.

3.3 Analysis of full waveform data

Based on the segmentation, the stem detection, and the known DTM all the points within a tree segment were subdivided into the three categories "stem points" below the base height, "ground points" and "crown points" representing the tree crown. Possible stems points in the tree crown were excluded by discarding all the points within the stem cylinder V_{stem}, where V_{stem} is defined by the 3D stem line g_{stem} as the centre line of the cylinder and the radius R = 1 m. Ground points were found within a height bound of 1 m to the DTM. Furthermore, I_i^c and W_i^c of the points were analysed with respect to the incident angle of the laser beam. Because of the scanning angle of 45^0 the maximum incident angle amounted to 22.5^0. Thus, mean values and standard deviations were calculated in an angle interval of 5^0 for the point classes given in Table 1 and are used in the following for visual analysis in Figures 4 to 10.

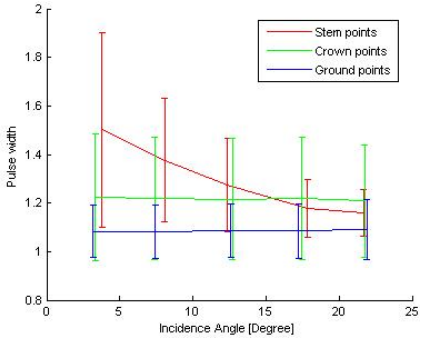

Figure 4. Mean pulse width and standard deviation (single and last points) for the three point categories

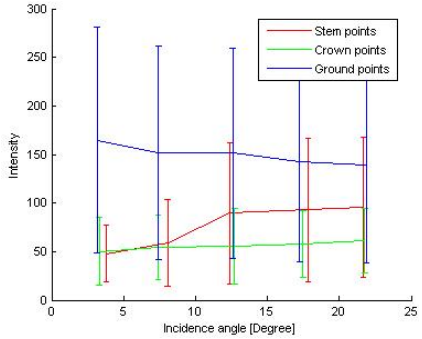

Figure 5. Mean intensity and standard deviation (single and last points) for the three point categories

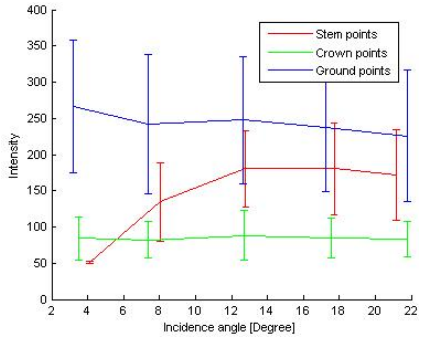

Figure 6. Mean intensity and standard deviation (single points) for the three point categories

In general, we found that roughly 75 % of the stem points are single and last points. Since ground points are also only composed by single and last points we focussed primarily on these point classes. The Figures 4 and 5 show for these point classes the mean values for pulse width and intensity and their standard deviations in dependence on the incident angle. Apparently, the ground points differ from stem points and crown points considerably. Both crown and ground points show no angle dependence. The undulating ground, the undergrowth, and the varying reflecting targets in the crown average the individual values for pulse width and intensity. As expected, the pulse width for the stem points decreases with increasing incident angle since with increasing incident angle the angle between laser beam and the normal to the stem surface gets smaller. This leads to a smaller broadening of the pulse.

Accordingly, the slight increase of the intensity with increasing incident angle can be interpreted the same way. Figure 6 focuses especially on the intensity of single points. Apparently, the three point categories differ fairly well for an angle range of 10^0 and 22.5^0. This was the only point class that indicated the best discrimination between the stem points and crown points. Most notably, ground points and crown points can be clearly separated. These results correspond with experiences of the study (Doneus et al., 2006), which recommends the use of intensity and pulse width along with point coordinates to generate a DTM from full waveform data.

We focus now on the important question in how far intensity and pulse width discriminate tree species. We restrict ourselves to coniferous and deciduous trees, which are the dominating trees in the study area. Crown points and stem points are assigned to the two tree species using the reference data. Again, the mean values and the standard deviation for I_i^c and W_i^c are analysed with respect to the incident angle. From Figure 7 we can conclude that the mean pulse width W_i^c of single crown points is different for coniferous and deciduous trees and is independent on the incident angle. Interestingly, we found that the difference in the pulse width was significant especially for single points. However, the difference of the mean intensity I_i^c was distinctive for all the four point classes, again without any dependence on the incident angle (Figure 8).

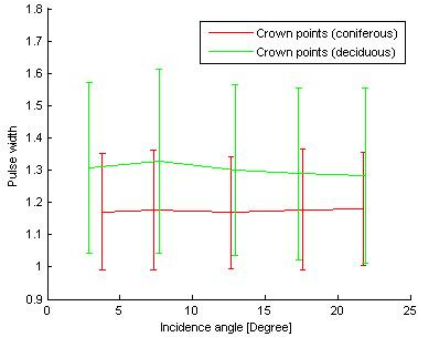

Figure 7. Mean pulse width and standard deviation (single points) for coniferous and deciduous crown points

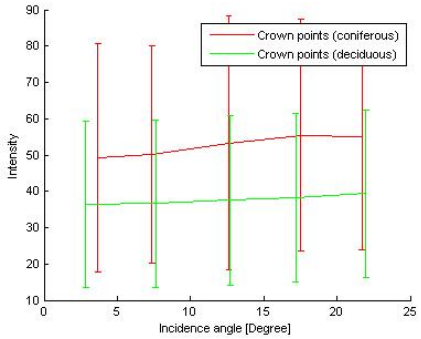

Figure 8. Mean intensity and standard deviation (all point classes) for coniferous and deciduous crown points

Finally, we concentrate on the stem points. The mean pulse width W_m^c is practically the same for the two tree species using all four point classes and decreases slightly with increasing incident angle (Figure 9). Apparently, the shape of coniferous and deciduous tree stems influences the pulse width the same way. Of course, the incident angle still plays a role likewise in Figure 4. Surprisingly, the mean intensity for single points is clearly different for coniferous and deciduous tree stems (Figure 10). Probably, the absorption and reflecting characteristics of stems have a clear impact on the mean intensity.

We have corrected the intensity of all point classes according to equation (2) assuming that the target size is equal or larger the laser footprint. This assumption is true for ground points and – probably – for most of the stem points. Since the target size of the crown points is not known we corrected them like stem or ground points.

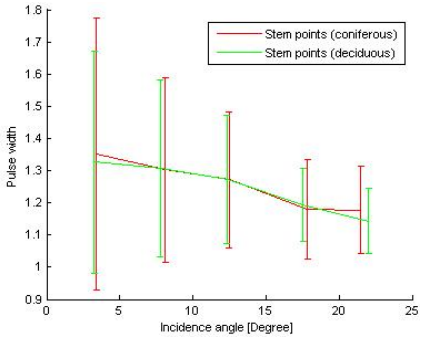

Figure 9. Mean pulse width and standard deviation (all point classes) for coniferous and deciduous stem points

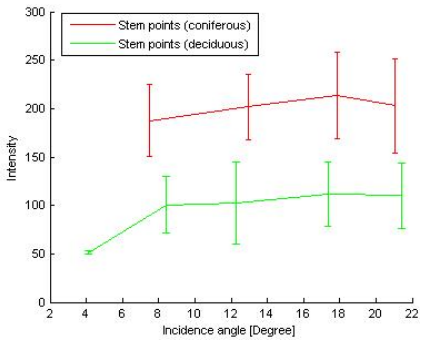

Figure 10. Mean intensity and standard deviation (single points) for coniferous and deciduous stem points

4. DISCUSSION

Conceptually, the presented approach to single tree detection from airborne LIDAR data goes one step further by using the CHM and additional information inside the tree. It leads to an improvement of the detection rate of single trees in the intermediate and upper forest layer by detecting tree stems. This refinement of the detection rate could be expected since (i) in many cases neighbouring trees do not appear as two clear maximums in the raw data and (ii) the smoothing of the CHM blurs the maximums. Apparently, as already pointed out by some other authors (e.g. Solberg et al., 2006), the smoothing of the reconstructed CHM influences the quality of the single tree detection considerably. The second advantage of the presented method is that the position of detected trees is improved. This is also not very surprising since the intersection of the detected tree stem with the DTM must be more precise than the tree position derived from the CHM maximum. Thirdly, the stem detection checks the hypothesis of a stem position which has been derived from the CHM. The restrictions of the approach are that only trees in the upper and intermediate forest layer can be additionally detected. It fails in the under layer where stem hits are rare and stems points can not be clearly clustered. Moreover, so far we have not implemented to go back to the

raw data and to find a new segmentation of the tree crowns using the stem information.
The analysis of the waveform data shows that the intensity and pulse width can be advantageously used for the discrimination of crown, stem and ground points, if the reflections are distinguished with respect to their position in the waveform. This information can be helpful for a true 3D segmentation. Moreover, we found that the mean pulse width and the mean intensity are characteristic for coniferous and deciduous trees. Thus, these experiences are very useful for (i) a DTM generation in forest areas, (ii) an improvement of the stem detection, (iii) and a tree species classification. For instance, ground or stem points can be more reliably detected using the intensity and pulse width as explained in the Figures 4, 5 and 6. Furthermore, the classification of coniferous and deciduous trees in leaf-off situation can advantageously use features that are composed from the mean intensity and pulse width of the tree crowns. If stem points can be detected the mean intensity of single points is the most meaningful feature. The pulse width of stem points is useless for classification purposes.

5. CONCLUSIONS

The study presents a novel single tree detection based on a combined surface reconstruction and stem detection. The results attained in heterogeneous forest types show that the detection rate and position of single trees can be improved in the upper and intermediate layer. Based on the stem detection the analysis of the waveform data shows a clear dependency of the intensity and the pulse width with respect to crown points, stem points, ground points, and tree species, resp. Future research should be focussed on the improvement of the segmentation of the tree crowns using the stem information.

ACKNOWLEDGEMENTS

We thank Dr. Marco Heurich and the Administration of the Bavarian Forest National Park for their productive contributions and for giving us the opportunity to use their remote sensing test sites.

REFERENCES

Brandtberg, T., 2007, Classifying individual tree species under leaf-off and leaf-on conditions using airborne lidar. *ISPRS Journal of Photogrammetry and Remote Sensing*, 61, pp. 325 – 340.

Doneus, M., Briese, C., 2006, Full-waveform airborne laser scanning as a tool for archaeological reconnaissance. In: Campana S., Forte M. (eds.), From Space to Place. *Proceedings of the 2nd International Conference on Remote Sensing in Archaeology*. BAR International Series 1568, 2006, 99-106.

Heijden, F. van der, Duin, R.P.W., Ridder, D. de, Tax, D.M.J., 2004. *Classification, parameter estimation and state estimation – An engineering approach using MATLAB.* John Wiley & Sons Ltd, The Attrium, southern Gate, Chichester, West Sussex PO19 8SQ, England.

Heurich, M., 2006, Evaluierung und Entwicklung von Methoden zur automatisierten Erfassung von Waldstrukturen aus Daten flugzeuggetragener Fernerkundungssensoren. *Schriftenreihe des Wissenschaftszentrums Weihenstephan für Ernährung, Landnutzung und Umwelt der Technischen Universität München und der Bayerischen Landesanstalt für Wald und Forstwirtschaft,* Forstlicher Forschungsbericht München, Nr. 202, ISBN 3-933506-33-6. http://meadiatum2/ub.tum.de/. (Accessed February 18, 2007)

Holmgren, J., Persson, Å., 2004, Identifying species of individual trees using airborne laser scanner. *Remote Sensing of Environment* 90 (2004) 415-423.

Hyyppä, J., Kelle, O., Lehikoinen, M., Inkinen, M., 2001. A segmentation-based method to retrieve stem volume estimates from 3-D tree height models produced by laser scanners. *IEEE Transactions on Geoscience and remote Sensing,* 39:969-975.

Hyyppä, J., Hyyppä, H., Litkey, P., Yu, X., Haggren, H., Rönnholm, P., Pyysalo, U., Pikänen, J., Maltamo, M., 2004, Algorithms and methods of airborne laser scanning for forest measurements. *Proceedings of the ISPRS working group VIII/2 Laser-Scanners for Forest and Landscape Assessment,* Volume XXXVI, PART 8/W2, 3 – 6th October, Freiburg, pp. 82 – 89.

Jutzi B., Stilla U. 2005. Waveform processing of laser pulses for reconstruction of surfaces in urban areas. *In: Moeller M, Wentz E (eds) 3th International Symposium: Remote sensing and data fusion on urban areas, URBAN 2005. International Archives of Photogrammetry and Remote Sensing.* Vol 36, Part 8 W27.

Krzystek, P., Wild, D., 1992, Experimental accuracy analysis of automatically measured digital terrain models. *Robust Computer Vision: Quality of vision algorithms.* Förstner, Ruhwiedel (ed.). Wichman Verlag, Karlsruhe, pp. 372 -390.

Persson, A., Holmgren, J. and Söderman, U., 2002. Detecting and measuring individual trees using an airborne laserscanner. *Photogrammetric Engineering & Remote Sensing* 68(9), pp. 925–932.

Pyysalo, U., Hyyppä, H., 2002. Reconstructing Tree Crowns from Laser Scanner Data for Feature Extraction. In *ISPRS Commission III, Symposium 2002 September 9 - 13, 2002, Graz, Austria*, pages B-218 ff (4 pages).

Reitberger, J., Krzystek, P., Stilla, U. 2006. Analysis of Full Waveform Lidar Data for Tree Species Classification. *Symposium ISPRS Commission III "Photogrammetric Computer Vision" PCV06*, 20 – 22th September, Bonn, Germany.

Solberg, S., Naesset, E., Bollandsas, O. M., 2006. Single Tree Segmentation Using Airborne Laser Scanner Data in a Structurally Heterogeneous Spruce Forest. *Photogrammetric Engineering & Remote Sensing,* Vol. 72, No. 12, December 2006, pp. 1369-1378.

Vincent, L., Soille, P., 1991, Watersheds in Digital Spaces: An Efficient Algorithm Based on Immersion Simulations. *IEEE Transactions of Pattern Analysis and Machine Intelligence*, Vol. 13, No. 6, June 1991, pp. 583-598.

Wagner, W., Ullrich, A., Ducic, V., Melzer, T. and Studnicka, N., 2006, Gaussian decomposition and calibration of a novel small-footprint full-waveform digitising airborne laser scanner. *ISPRS Journal of Photogrammetry and Remote Sensing*, 60, pp. 100-112